Modeling of electron transport in nanoribbon devices using Bloch waves

Akash A. Laturia[1], Maarten L. Van de Put[1], Massimo V. Fischetti[1], and William G. Vandenberghe[1]

[1]*The University of Texas at Dallas, 800 W. Campbell Rd., Dallas, Texas 75080, USA*

Email: wxv1010120@utdallas.edu / Phone: (972)-883-5793

One-dimensional (1D) materials present the ultimate limit of extremely scaled devices by virtue of their spatial dimensions and the excellent electrostatic gate control in the transistors based on these materials. Among 1D materials, graphene nanoribbon (a-GNR) prove to be very promising due to high carrier mobility and the prospect of reproducible fabrication process [1]. Two popular approaches to study atomistically the electronic properties expand the wavefunction on either a plane-wave basis set, or through the linear combination of localized atomic orbitals. The use of localized orbitals, especially in the tight-binding (TB) approximation, enables highly scalable numerical implementations. Through continuous improvements in methods and computational capabilities, atomistically describing electronic transport in devices containing more than thousands of atoms has become feasible. Plane waves, while not as scalable, are very popular as the basis of accurate *ab-initio* software [2]. However, for modeling of transport through larger devices, the computational burden prohibits the direct use of a plane wave basis [3]. Here, we demonstrate a study of the transport characteristics of nanoribbon-based devices using a hybrid approach that combines the benefits of plane waves while retaining the efficiency provided by the TB approximation.

For our hybrid method, we discretize the device structure in different supercells as shown in Fig. 1. The device Hamiltonian, from which we determine electron transport properties, can be separated as follows: $H(\mathbf{r}) = H_{\text{crystal}}(\mathbf{r}) + V_{\text{external}}(\mathbf{r})$. The crystal part of the Hamiltonian ($\text{H}_{\text{crystal}}(\mathbf{r})$) is periodic and varies significantly on the atomic scale, within one supercell, whereas the external potential ($\text{V}_{\text{external}}(\mathbf{r})$) varies smoothly over the entire device. As $\text{H}_{\text{crystal}}(\mathbf{r})$ remains constant and $\text{V}_{\text{external}}(\mathbf{r})$ changes during the successive iterations of the transport solver, we expand the wavefunctions in the device on a select set of solutions of $\text{H}_{\text{crystal}}(\mathbf{r})$ in the supercells, *i.e.*, the Bloch waves of that supercell. The Bloch waves are calculated to high accuracy using a plane-wave basis method, while the TB-like character of the large-scale system provides excellent scalability. Expanding the wavefunction on these Bloch waves captures the atomic-scale variations within the supercells. A partition-of-unity method (PUM) [4] is used to "stitch" the wavefunctions from different supercells together, yielding a TB-like Hamiltonian. The PUM effectively describes the large-scale behavior of the system. Having constructed the Hamiltonian, the open system is modeled using the Quantum Transmitting Boundary Method (QTBM) [5]. Since we have access to the plane wave expansion of our Bloch waves, we are able to reconstruct the full 3D electron density from the solutions of the discretized Schrödinger equation. The Hartree potential is determined self-consistently with the electron density using the Poisson equation. After the self-consistent calculation of the Schrödinger-Poisson system, we calculate the ballistic transport properties of the device under study. Unlike a fully delocalized plane-wave basis set method, our method scales well, as it scales with the number of Bloch waves instead of the number of plane-waves. Thus we retain most of the benefits of the plane wave method while reducing the computational burden by at least two orders of magnitude.

Here we showcase ballistic transport studies in a 1.35 nm wide a-GNR (armchair configuration) using the Bloch waves based electron transport model. The device under study is illustrated in Fig. 2. Each supercell consists of 24 atoms whereas the device consists of 960 atoms in total. We use an all-around gate with vacuum as the dielectric. The constructed full band-structure is shown in Fig. 3. The entire energy spectrum is constructed based on the Bloch waves at two k-points namely, the center and the boundary of the 1D Brillouin zone. The use of two distinct k-points avoids spurious solutions due to the use of a finite basis set. The Bloch waves that constitute the basis set are computed using the empirical pseudopotential method (EPM). The computed bandstructure (Fig. 3) when compared against the bands obtained using the EPM shows an agreement throughout within 25 meV thereby validating our approach for these structures. To illustrate the reconstruction of full real-space properties using our method, the 3D potential profile and the electron density profile through the device in the off-state are presented in Fig. 4. The computed current-voltage (I-V) curve for the monolayer a-GNR is shown in Fig. 5. We observe that this a-GNR FET provides an $I_{\text{on}}/I_{\text{off}}$ ratio of about 10^6 with a subthreshold slope on the order of 120 meV/decade. This can be attributed to the very short (2nm) gate length. In order to investigate the effect of multiple layers on the electron transport properties, a 1.35 nm-wide bilayer-GNR has been studied using the same model. These results are shown in Fig. 6.

The work presented here is supported by the NSF Grant No. 1710066.

[1] X. Li, X. Wang, L. Zhang, S. Lee, H. Dai, Science **319**, 1229 (2008).

[2] Kresse, G. & Furthmüller, J., Phys. Rev. B **54**, 11169–11186 (1996).

[3] J. Fang, W. G. Vandenberghe, B. Fu, and M. V. Fischetti, J. Appl. Phys. **119**, 035701 (2016).

[4] Melenk JM, Babuška I., Computer Methods in Applied Mechanics and Engineering 1996; **39**:289–314.

[5] C. S. Lent and D. J. Kirkner, J. Appl. Phys. **67**, 6353(1990).

978-1-5386-3028-0/18/$31.00 ©2018 IEEE

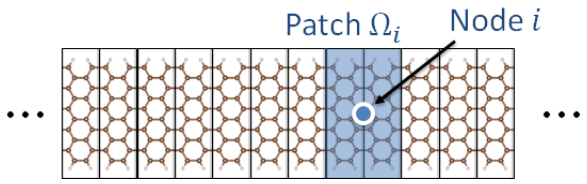

Fig. 1: Schematic representation of the discretized device. The patch Ω_i represents the region spanned by the supercell at node i. The electron wavefunctions are calculated in each supercell, and then stitched together using a PUM on the patches of each node as indicated.

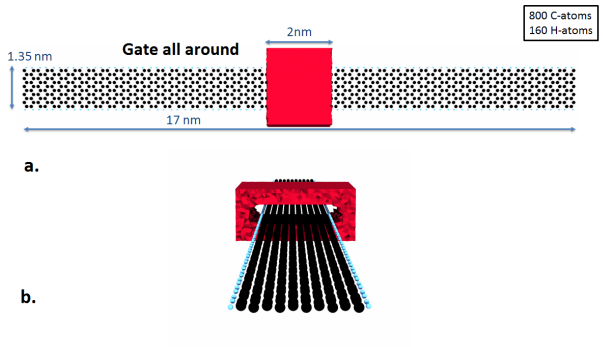

Fig. 2: Schematic of the 5 a-GNR based device with gate all around geometry. a. Top view of the device. b. Side view of the device. Source and drain are n-doped with a doping density of 4.509 $\times 10^8$/nm whereas the channel region is p-doped with the same doping density.

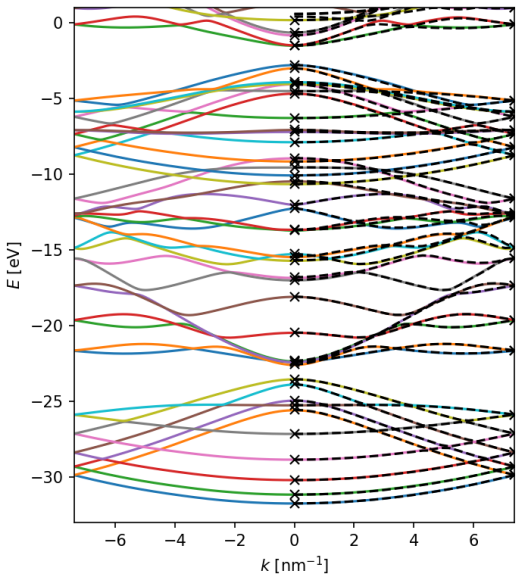

Fig. 3: The reconstructed bandstructure from the Bloch waves superimposed on the EPM bandstructure. The colored lines represent the reconstructed bands whereas the dashed lines represent the bands obtained using EPM. The reconstruction is based on the Bloch waves at the center and right-edge (indicated by x). The bands match well within 25 meV thereby validating the reconstructed bands.

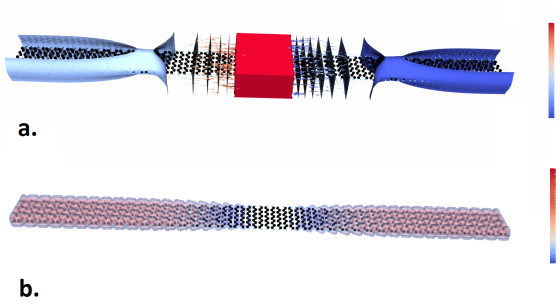

Fig. 4: a. Potential iso-energy surfaces and electric field vectors in the off-state. b. Electron density profile through the device in the off-state.

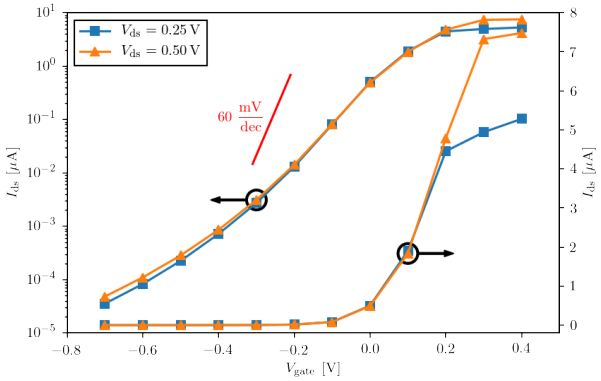

Fig. 5: GNR: I-V characteristics. The calculated subthreshold slope for the device is of the order of 120 meV/decade

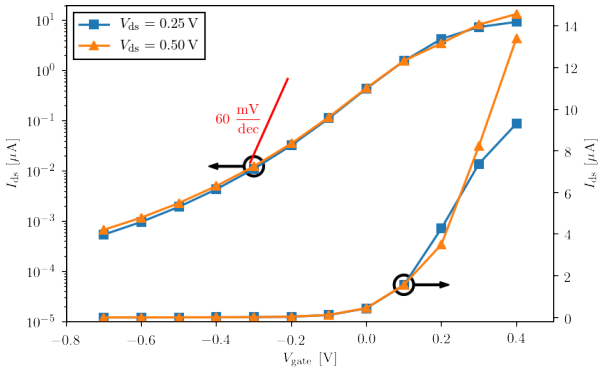

Fig. 6: Bilayer GNR: I-V characteristics. The calculated subthreshold slope for the device is of the order of 175 meV/decade. The gate control worsens in the bilayer GNR as compared to its monolayer counterpart.

978-1-5386-3028-0/18/$31.00 ©2018 IEEE